Thallium-201 Myocardial Imaging: Characterization of the ECG-Synchronized Images

Glen W. Hamilton, Kenneth A. Narahara, Gene B. Trobaugh, James L. Ritchie, and David L. Williams

Veterans Administration Hospital and University of Washington Seattle, Washington

Electrocardiographic synchronization of Tl-201 myocardial scintigrams provides images free of blurring due to the motion artifact induced by myocardial contraction. The current study was performed to characterize the qualities and technique of synchronized thallium imaging. Twenty-five studies were performed in 18 patients. Initially, standard nonsynchronized images were obtained with a high-resolution collimator in the anterior, left anterior oblique (30°, 45°, and 60°), and left lateral positions. Next, a 30-min ECG-synchronized image was acquired with a high-sensitivity collimator in the 45° left anterior oblique view. Fifty-millisecond images of the cardiac cycle can be viewed in cine mode, or end-diastolic and end-systolic images can be constructed using predefined criteria and/or a region-of-interest analysis to detect motion. With the 30-min imaging time, motion-free images with adequate counts were routinely obtained. The synchronized motion-free images resolved the myocardium more clearly and defects were more readily apparent than with the standard nonsynchronized images. Systolic myocardial thickening and wall motion could be appreciated by visual inspection or by computer analysis. This study demonstrates that image quality is enhanced by synchronized imaging and that wall motion can be assessed. Due to the longer imaging time required for synchronized imaging, it is not possible to obtain the multiple views usually obtained with standard imaging. The data presented demonstrate, however, that motion-free pictures of end-diastole alone could be obtained in much less time. It remains undetermined whether fewer ECG-synchronized views, rather than more views without synchronization, would improve lesion detectability.

J Nucl Med 19: 1103–1110, 1978

Electrocardiographic (ECG) gating or synchronization of gamma images collected over a period of time can be used to produce static images free of motion artifact at end-diastole or end-systole. Recently, computer techniques have been developed to acquire, analyze, and immediately display the data as static images or in a sequential cine format (*1,2*). Most commonly, these techniques have been used to collect images of the cardiac chambers following administration of a radionuclide distributed in the blood pool. Alderson, Wagner, and associates (*3,4*) demonstrated that the same techniques could be applied to thallium-201 myocardial images.

We have investigated this technique in detail to determine the characteristics of the images so obtained and to develop logic for obtaining maximal data with minimal imaging time.

Received Sept. 26, 1977; revision accepted Apr. 21, 1978.

For reprints contact: Glen W. Hamilton, Chief, Nuclear Medicine Section (115), Veterans Administration Hospital, 4435 Beacon Ave. So., Seattle, WA 98108.

Initial studies indicate that this approach is useful for the removal of motion artifact inherent in non-synchronized studies and for the direct study of left-ventricular wall motion and thickening.

MATERIALS AND METHODS

Twenty-five Tl-201 myocardial imaging studies were performed in 18 patients—ten at rest and 15 following an injection at maximal exercise—using 1.5–2.0 mCi of Tl-201 for each study. Imaging was performed with a gamma camera using an 18,000 parallel-hole, high-resolution, 140-keV collimator and a FWHM energy window centered over the mercury x-rays. Scintiphotos were obtained with 300,000 to 400,000 counts, in the anterior, left anterior oblique (30°, 45°, 60°) and left lateral positions. The same system was then equipped with a low-energy, high-sensitivity collimator to acquire a single 30-min ECG-synchronized image in the 45° left anterior oblique view. All scintillation data were acquired and stored on a dedicated computer system. During collection of the ECG-synchronized data, a pulse synchronous with the R wave was collected, and the computer stored each sequential 50-msec segment of the cardiac cycle in core and added the corresponding 50 msec of each subsequent cardiac cycle to the appropriate core location. The total number of cardiac cycles collected varied, being equal to 30 min multiplied by the patient's heart rate (about 2,000 cycles per study). During the imaging period, analog scintiphotos of end-diastole and end-systole were also obtained using a commercially available ECG-gating device to unblank the oscilloscope at predetermined intervals.

Two methods of constructing end-diastolic and end-systolic images from the ECG-synchronized data were investigated. In the first, the timing of end-systole and end-diastole were estimated from a graph based on 16 left-ventricular time-volume curves obtained by contrast ventriculography (*5,6*). This graph, shown in Fig. 1, allows the approximate prediction of the timing of various phases of the cardiac cycle for heart rates varying between 60 and 85 per minute. The second method employed a region of interest placed over the central area of decreased activity in the left anterior oblique (LAO) Tl-201 image obtained during the first 50 msec following the ECG R wave (Fig. 2). The time-activity curve for this region throughout the entire cardiac cycle was then generated. As the myocardium contracted toward the center of the image during systole, the activity in the center of the image increased, as indicated in the diagram in Fig. 2. Various limits were then employed to select end-diastole and end-systole (see below) from the time-volume relationship (Fig. 1) and the time-activity curve (Fig. 2).

RESULTS

The ECG-gated images were satisfactory in all 25 studies. The 30-min collection period was somewhat lengthy and even though all patients completed the study, it seemed unlikely that longer imaging times would be clinically practical. The ECG-gated analog images obtained directly from the camera were generally marginal due to the short windows selected for end-diastole (80 msec) and end-systole (50 msec). The data presented below suggest, however, that it would be possible to expand these time intervals considerably with resultant improvement in counts per image.

The total image counts collected by the camera during the synchronized imaging study varied from 1.2–1.6 million. Each single 50-msec image segment of the cardiac cycle stored in the computer contained

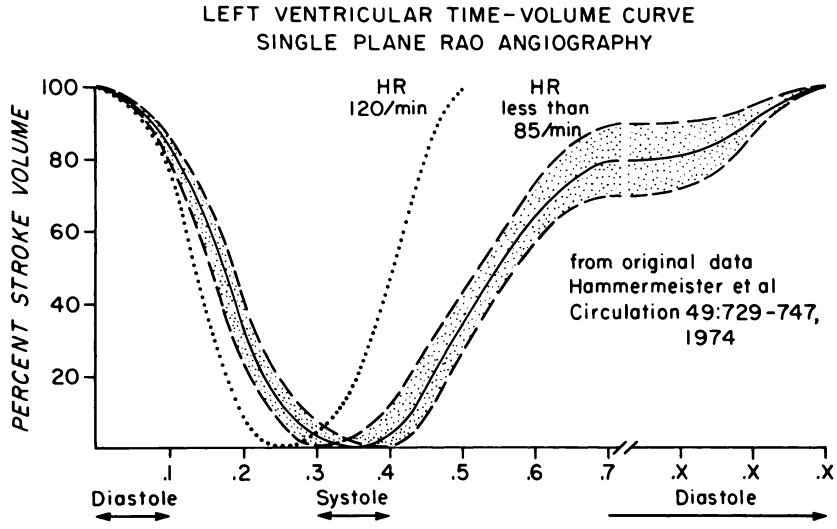

FIG. 1. Left-ventricular time-volume relationships determined by contrast cineangiography. Time scale is expressed in seconds after R wave. With heart rates between 60 and 85 per minute, minimum volume (end-systole) occurs between 0.3 and 0.4 sec after R wave. Thus, selection of the 0.1-sec interval between 0.3 and 0.4 sec will closely approximate end-systole. Note that as R-R interval decreases (heart-rate increase), timing of end-systole changes only slightly whereas period of diastole is shortened considerably. Based on this relationship, one can arbitrarily assign periods of diastole and systole that will minimize motion artifact.

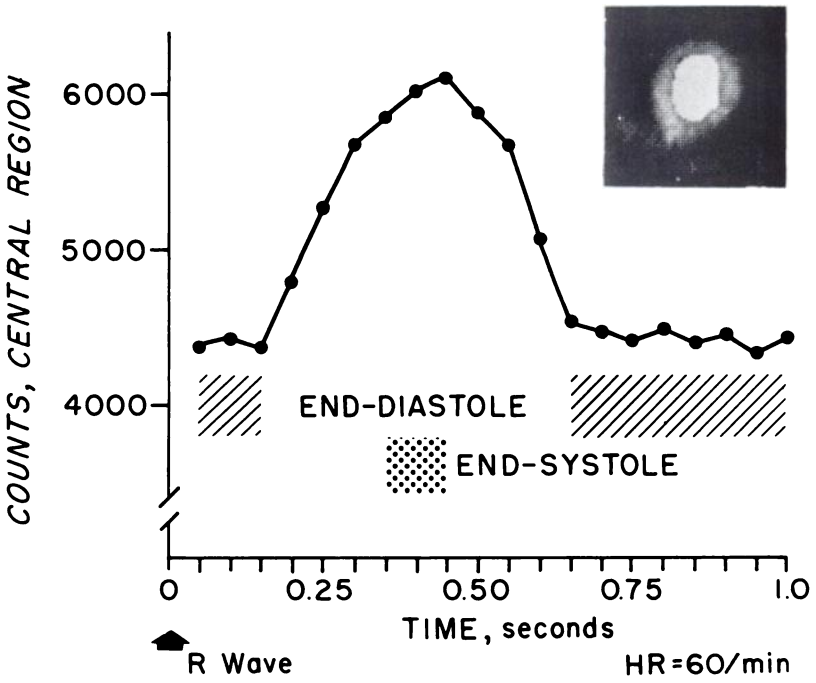

FIG. 2. Method for determining end-diastole and end-systole from ECG-synchronized thallium images. Central region of interest is traced by light pen over central area of decreased activity in LAO view. A time-activity curve is then generated. As ventricle contracts, more activity moves centrally and counts in central region increase. End-systole (dots) is represented by peak counts, and end-diastole (cross-hatched) by plateau of activity immediately after R wave and at end of cardiac cycle. Cross-hatched region defined as end-diastole includes initial portion of systole before ejection begins.

40,000 ± 7,000 counts (range 31,000–52,000)*.

The information content of a single 50-msec frame of data collected immediately following the R wave (end-diastole) is shown in Fig. 3. While the left and right ventricular walls are easily discernible, the image is of poor quality due to the low number of recorded events. The addition of one or more 50-msec frames occurring at or near end-diastole minimized the effect of poor imaging statistics without inducing motion artifact and hence improved image quality (Fig. 3). Images of approximately 100,000 counts appeared visually satisfactory, and although image quality improved perceptibly with each addition of a 50-msec frame (Fig. 3), the improvement noted is less with each subsequent addition.

Comparison of standard and synchronized images. Figure 4 shows a comparison between standard nongated images (with high-resolution collimator) and R-wave-synchronized images taken with a high-sensitivity collimator. The motion artifact in the standard unsynchronized images is quite apparent and causes blurring of the image in all areas. The loss of resolution is especially prominent at the outer margin of the ventricular cavity and the outer edge of the ventricular myocardium. The standard unsynchronized image was smaller than the end-diastolic and larger than the end-systolic R wave

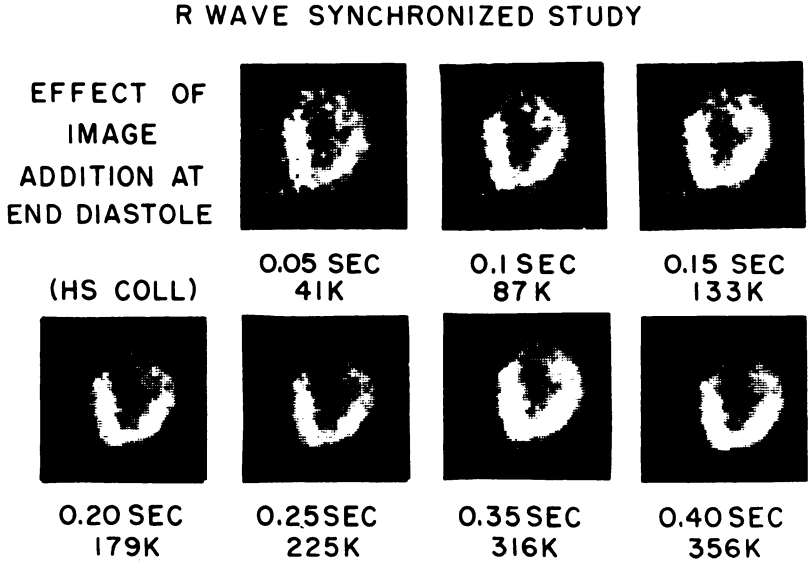

FIG. 3. Image frames at end-diastole (high-sensitivity collimator). Images are from study shown in Fig. 2, and represent addition of those frames defined as end-diastole in that figure. Image quality improves perceptably from 41 K to 133 K counts per image, but less so as additional frames are added.

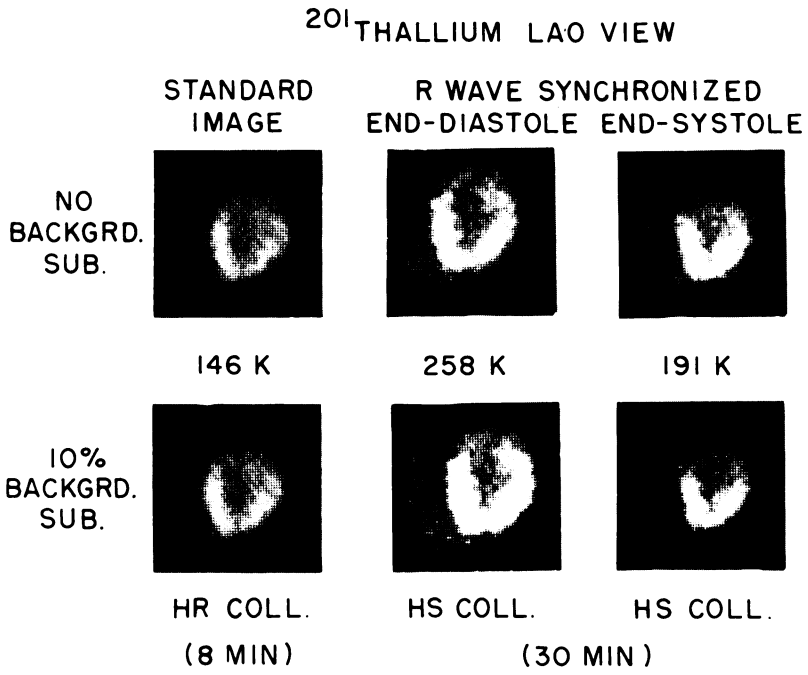

FIG. 4. Comparison of standard non-synchronized and synchronized images. Blurring due to motion artifact is readily apparent in standard image.

synchronized image. Overall, the configuration or pattern of the unsynchronized image corresponded most closely to the end-diastolic R wave synchronized image. This is consistent with the relatively longer time spent in diastole compared with systole at normal heart rates (see Fig. 1).

The analog scintiphotos collected by unblanking the oscilloscope at predetermined times corresponding to end-diastole and end-systole were essentially similar to those collected by and displayed on the computer system, although each contained fewer counts per image as noted above.

Wall motion. ECG-synchronized imaging also provided an evaluation of wall motion from the Tl-201 study. Wall motion was displayed by subtracting the end-systolic from the end-diastolic image after appropriate normalization to correct for the different numbers of counts in the images (Fig. 5). The wall-motion image shown is from the patient depicted in Fig. 4, and is normal, since he had normal coronary arteries and left-ventricular wall motion by contrast angiography. The apparent lack of motion in the anteroseptal and medial inferior myocardium is due to the combined effects of contraction toward the center of the cardiac mass and movement of the entire ventricle from left to right and anteriorly during systole. The same effect has been demonstrated independently by contrast cineangiography in our laboratory (G. B. Trobaugh, unpublished data). Close inspection of Figs. 4 and 5 also reveals that the posterior wall appears thicker than the anterior wall on the unsynchronized images (Fig. 4). This is not apparent on the end-diastolic or the end-systolic images. Furthermore, the wall-motion images (Fig. 5) show that this is the region of maximal cardiac-muscle motion. Both observations suggest that the thicker appearance of the posterior wall is in fact a motion artifact in this particular study.

Relative wall motion and thickening of the left-

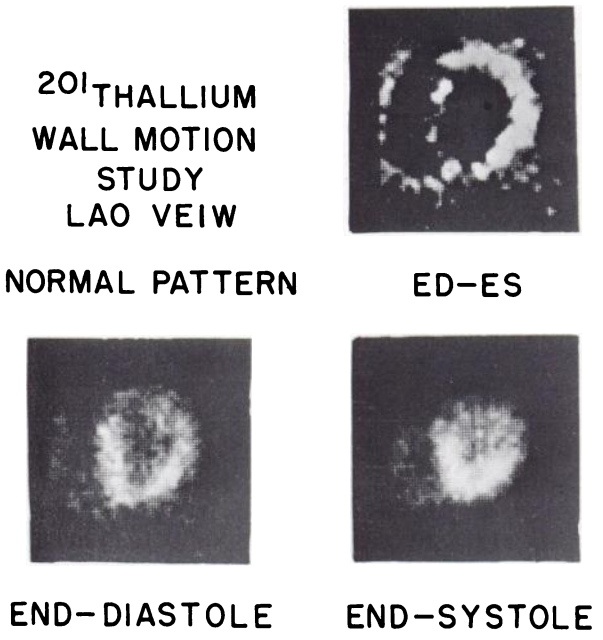

FIG. 5. Wall-motion study. End-systolic image is subtracted from end-diastolic image; residues indicate regions of myocardial motion. Much greater motion is noted in posterior wall than anteriorly due to movement of whole left ventricle anteriorly during systole.

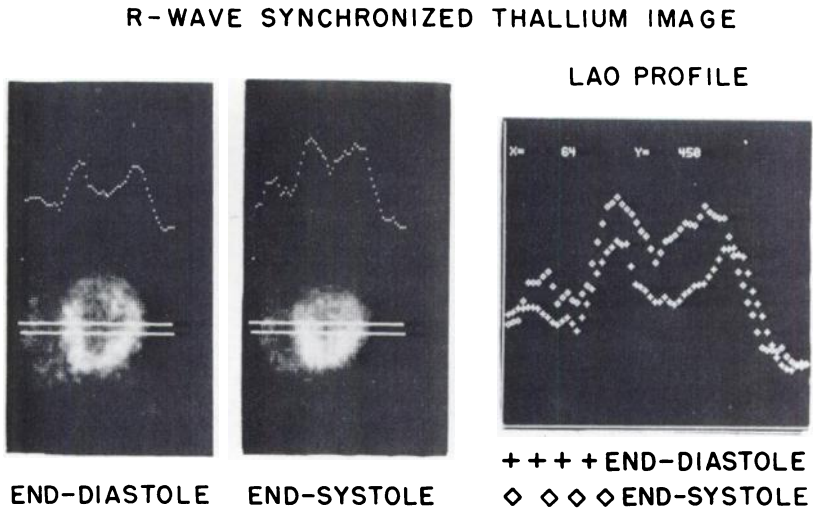

FIG. 6. Profile wall-motion analysis. Both anterior and posterior ventricular walls thicken during systole. Movement anteriorly is noted in posterior wall, whereas anterior wall remains relatively stationary.

ventricular myocardium can also be displayed graphically, as shown in Fig. 6. The images are the same as in Figs. 4 and 5. The changes in the profile curves demonstrate thickening of the ventricular walls (right ventricle, anterior left ventricle, and posterior left ventricle) during systole, as is evidenced by widening of the peaks over the walls and increased counts per channel. Note also that the peaks for the right ventricle and the posterior left ventricle moved toward the center, whereas the anteroseptal left-ventricular wall remained relatively stationary, confirming the validity of the wall-motion observation noted in Fig. 5 above.

Figure 7 illustrates the standard nonsynchronized as well as the R wave synchronized images of a patient with a documented small inferior myocardial infarction. The composite images show a small inferior perfusion defect best seen on the image with 10% background subtraction. The R wave synchronized images (particularly end-systole) clearly show this to be an area of inferior muscle thinning. Failure of the region of the ventricle to contract during systole is documented by subtraction of the end-systolic from the end-diastolic image (Fig. 8). Note also that the anteroseptal region shows more motion than that noted in the normal study of Fig. 5. In our

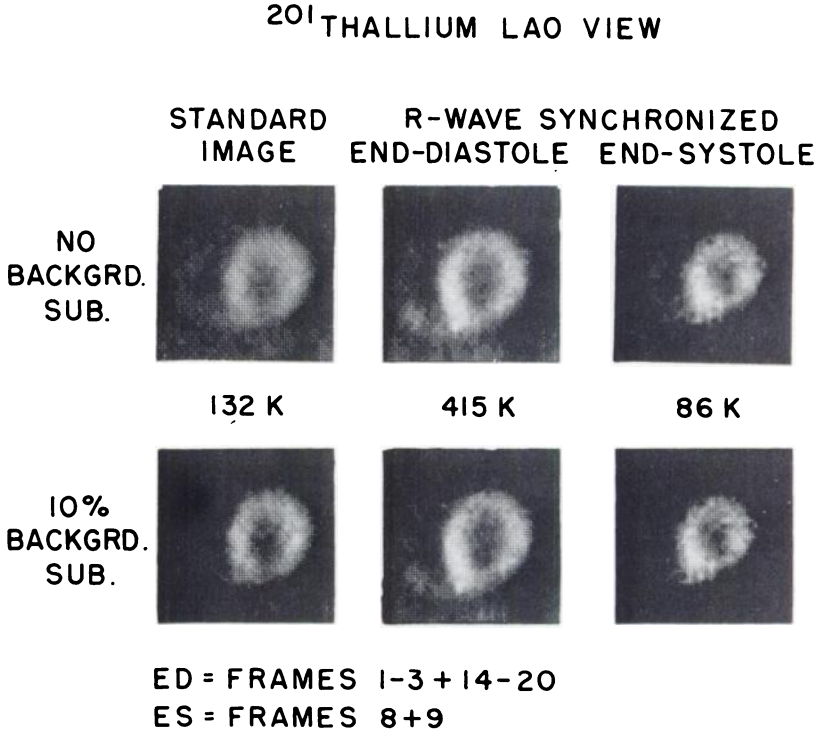

FIG. 7. Comparison of standard and synchronized images in patient with previous inferior myocardial infarction. Standard images shown an inferior defect. Synchronized images (particularly end-systole) show this to be due to thinning of inferior wall.

experience, increased anteroseptal motion frequently accompanies a contraction abnormality in another region.

Selection of end-diastole and end-systole. As mentioned earlier, selection of end-diastole and end-systole was based on two methods. Figure 1 shows the graph constructed from 16 time-volume curves obtained by contrast angiography. For each patient, the end-diastolic volume was normalized to 100% and the end-systolic volume to 0%. In the 15 patients with heart rates between 60 and 85 per minute, the timing of end-systole was similar, varying from 0.30 to 0.40 sec following the R wave. The shaded band in Fig. 1 represents the mean percentage volume change and the range of this measurement. A single patient with tachycardia (120 per minute) is shown for comparison. Note that while the time from the R wave to end-systole shortens slightly, the major change with increasing heart rate is more rapid ventricular filling and marked shortening of diastole.

From this sample (Fig. 1), it is possible to predict the approximate timing of images corresponding to end-diastole and end-systole. Images from 0–0.10 sec after, and more than 0.70 seconds following, the R wave will be within 20% of maximal diastolic volume; images from 0.30–0.40 sec will be within 10% of minimal systolic volume. If the limit for end-systole is increased to 20%, all images from about 0.27–0.45 sec following the R wave would be accepted as representing end-systole.

In the second method, time-activity curves were generated by placing a region of interest over the central lucent area (Fig. 2) to provide a more direct measure of myocardial motion as detected by the imaging system. The temporal similarities between the time-volume curve (Fig. 1) and the time-activity curve (Fig. 2) are apparent. Since muscle motion and volume change are coupled functions, one would anticipate this result. In 12 of 18 patients, the time-activity curve for the central region was essentially like that shown in Fig. 2, all showing a steep rise to a single maximum point and a rapid decline to diastole. All patients in the group had normal or only moderately reduced left-ventricular ejection fractions (>0.35). In the six patients with low ejection fractions (<0.35), the increase in central activity during systole was less pronounced and the peak activity poorly defined.

Selection of end-diastole and end-systole from the time-activity curve (Fig. 2) and from the time-volume relationship (Fig. 1) was performed in all cases with both 10% and 20% limits†.

With the time-activity method, 10% limits usually included two frames (100 msec) at end-systole and from two to eight frames at end-diastole. With 20% limits, motion artifact become noticeable in the end-systolic image, as shown in Fig. 9. In this example, 10% limits at end-systole included frames 8 and 9, while 20% limits included four frames (Trobaugh, and *8–10*). The latter limits show slight blurring due to motion (right-hand image, Fig. 9) compared with the 10% limit range (center image, Fig. 9). In this case, no additional frames were selected for end-diastole with the 20% limits than with the 10% limits; thus the images were identical.

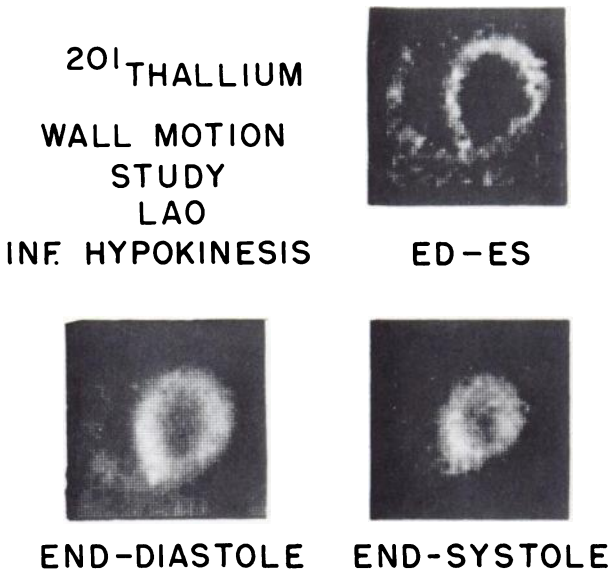

FIG. 8. Wall-motion study in patient with inferior infarction. Inferior wall has decreased motion.

In general, selection of end-diastole and end-systole from the time-volume relationship shown in Fig. 1 resulted in images very similar to those selected with the time-activity method. Several differences were noted. First, it is apparent from Fig. 1 that 10% limits with this method will include only the initial frame from 0–50 msec and the last 50-msec frame of diastole, whereas in each case, 10% limits with the time-activity method included at least four frames (and usually more) at end-diastole. The use of 20% limits with the time-volume method included the initial two frames (0–100 msec) and all frames after 0.7 seconds as end-diastole. As noted above, this corresponds closely to the number of frames included with 10% limits using the time-activity method. At end-systole, the methods were virtually identical; 10% limits usually included two frames, 20% usually four frames. As above, 20% limits with this method caused blurring due to motion at end-systole.

DISCUSSION

This study clearly documents the feasibility of

R wave synchronized Tl-201 imaging. The technique appears to offer several attractive features.

First, the synchronized image may provide improved resolution and improved lesion detectability by removing the motion artifact. From the data presented here, it is apparent that relatively motion-free images at end-diastole alone could be obtained in much less time than the 30 min required here to obtain images throughout the cardiac cycle. For instance, from the time course of ventricular volume (Fig. 1) and confirmed by motion in the R wave synchronized images (Fig. 2), it is apparent that most motion occurs between 0.1 and 0.6 sec following the R wave. Between 0 and 0.1 sec, and between 0.6 sec and the next R wave, image data collected will have very little motion artifact. At a heart rate of 60/min, about 50% of the cycle is relatively motion free (this decreases to about one-third at a heart rate of 80/min). Thus, if the same collimator were used for both the standard and synchronized images, imaging time would be increased by a factor of only 2–3 in most patients. Use of a high-sensitivity collimator would result in synchronized image times less than or equal to the time required for standard images with a high-resolution collimator.

The second feature is the ability to assess wall motion and overall ventricular contraction in addition to myocardial perfusion. The display of regional wall motion is simple by subtraction techniques or profile analysis. Furthermore, the data can be viewed in cine mode, which may make subtle contractile abnormalities more readily apparent.

In addition, the ability of synchronization to give a semi-quantitative estimate of ventricular wall thickening may allow for a prediction of early left-ventricular dysfunction. Animal data (Trobaugh, and 7) indicate that a decrease in systolic wall thickening may be the first detectable change in an ischemic myocardium. Currently these data cannot be obtained in humans by any conventional method. Synchronized Tl-201 imaging then is potentially an early marker of latent ischemic heart disease, since wall thickening is easily determined from the count profiles in end-systole and end-diastole.

The collection of sufficient data to yield diagnostic images at any point throughout the entire cardiac cycle will take approximately 30 min per view (due to the relatively short duration of systole). It is doubtful that multiple synchronized views (anterior, LAO, lateral) of the entire cardiac cycle would be clinically feasible. A single R wave synchronized image following the standard three or four nonsynchronized views, however, is feasible and was well tolerated by the patients studied here. For practical purposes, this could be a substitute for blood pool imaging to assess resting ventricular wall motion. Alternatively, Alderson et al. (*4*) have demonstrated that synchronized and nonsynchronized images can be obtained simultaneously using a high-sensitivity collimator in only 10–15 min per view. Although their images have fewer counts, they report satisfactory image presentation for cine-mode viewing.

Our data were acquired and stored in a dedicated computer and time-activity analysis was performed to determine the true end-systolic and end-diastolic frames. However, the availability of the time-volume curves presented in Fig. 1 provides a simple means by which any laboratory with an ECG-gating device can produce images of comparable quality. Our observations indicate that the images produced by using the known time-volume curves to determine the timing of end-diastole and end-systole will approach the image quality as well as the actual framing as determined by the time-activity analysis.

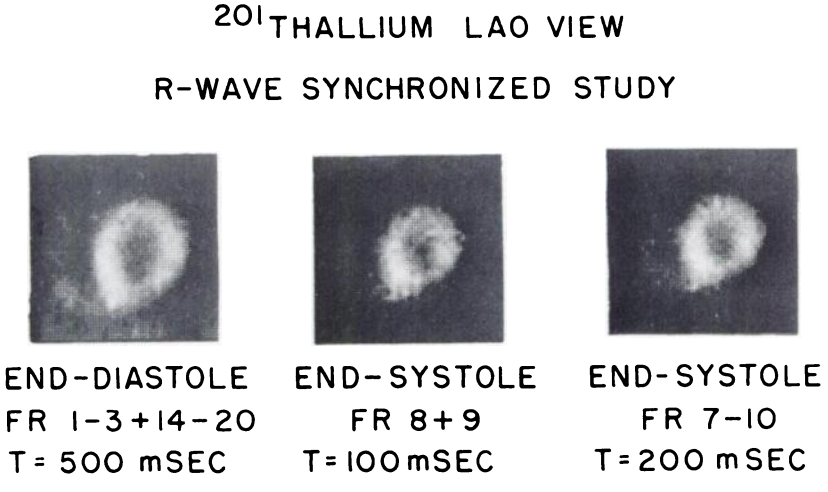

FIG. 9. Comparison of different limits for construction of end-diastole using time-activity method. The 10% and 20% limits both included the same number of frames for end-diastole. For end-systole, 10% limits included Frames 8 and 9, 20% limits included Frames 7–10. Some blurring due to motion is apparent on the 20%-limit, 4-frame image (right panel) compared with the 10%-limit, 2-frame image (center panel). T = time; FR = frame.

Note that the imaging protocol used in this study (a 30-min imaging time with a high-sensitivity collimator) was selected to produce high-quality images throughout the cardiac cycle. This was necessary to compare the end-diastolic and end-systolic images and for the analysis of wall motion. As noted above, these data permit the development of imaging protocols that would eliminate motion blurring by collection of images only at or near end-diastole, and would require much less than 30 min of imaging time. For several reasons we made no attempt to compare the detectability of regional perfusion defects on the standard against the synchronized images. Fifteen of the studies were postexercise, and redistribution of thallium, as shown by Pohost et al. (*9*), probably would have changed the myocardial thallium distribution by the time the synchronized images were performed (1–2 hr postinjection). Furthermore, the number of patients studied (18) precludes any significant statistical analysis of lesion detection with the two methods.

The differences between the high-resolution and high-sensitivity collimators should be noted. High-sensitivity collimators usually demonstrate more loss of resolution at depth compared with high-resolution collimators. Thus, during comparison of the standard and synchronized images, the apparent improvement is due to the combined effects of improved resolution due to removal of motion artifact, plus diminished resolution due to the use of the high-sensitivity collimator. The exact contribution of these two factors cannot be assessed from this study. For instance, ECG-gated studies employing a high-resolution or medium-resolution collimator could result in further improvement in resolution, even though fewer counts per image would be available.

In summary, this study characterizes ECG-synchronized imaging in terms of the timing and duration of motion during the cardiac cycle, the degree of improvement due to removal of motion, the number of counts needed to provide a satisfactory image, and the additional information available from the thallium images regarding wall motion. Although the present imaging protocol can be implemented clinically, further studies are needed to determine the optimum type of collimation and length of the imaging study.

FOOTNOTES

* The computer program used recorded and stored only from the central one-fourth to one-third of the total crystal surface.

† Example: For the time-activity method, counts in the central region reached a maximum of 6,000 during systole and a minimum of 4,000 during diastole. Ten percent of (6,000 − 4,000) = 200 counts. All images with central activity exceeding 5,800 counts defined as end-systole; all images with activity less than 4,200 counts defined as end-diastole. For the time-volume relationship (Fig. 1), 10% and 20% limits are read directly from the percentage scale on the vertical axis, as described in Methods.

REFERENCES

1. BACHARACH SL, GREEN MV, BORER JS, et al: A real-time system for multiimage gated cardiac studies. *J Nucl Med* 18: 79–84, 1977

2. FOLLAND ED, HAMILTON GW, LARSON SM, et al: The radionuclide ejection fraction: A comparison of three radionuclide techniques with contrast angiography. *J Nucl Med* 8: 1159–1166, 1977

3. WAGNER HN, LOTTER MG, DOUGLAS KH, et al: Cinematic display of regional function in nuclear imaging. *J Hopkins Med J* 142: 61–66, 1978

4. ALDERSON PO, WAGNER HN, GOMEZ-MOREIRAS JJ, et al: Simultaneous detection of myocardial perfusion and wall motion abnormalities by cinematic ^{201}Tl imaging. *Radiol*: in press

5. HAMMERMEISTER KE, BROOKS RC, WARBASSE JR: The rate of change of left ventricular volume in man. I. Validation and peak systolic ejection rate in health and disease. *Circulation* 49: 729–738, 1974

6. HAMMERMEISTER KE, WARBASSE JR: The rate of change of left ventricular volume in man. II. Diastolic events in health and disease. *Circulation* 49: 739–747, 1974

7. GOLDSTEIN S, DEJONG JW: Changes in left ventricular wall dimensions during regional myocardial ischemia. *Am J Cardiol* 34: 56–62, 1974

8. DEJONG JW, GOLDSTEIN S: Changes in coronary venous inosine concentration and myocardial wall thickening during regional ischemia in the pig. *Circ Res* 35: 111–116, 1974

9. POHOST GM, ZIR LM, MOORE RH, et al: Differentiation of transiently ischemic from infarcted myocardium by serial imaging after a single dose of Thallium-201. *Circulation* 55: 294–302, 1977